Qualifying an L5 SBAS MOPS Ephemeris Message to Support Multiple Orbit Classes

Tyler Reid, Todd Walter, & Per Enge
Stanford University

BIOGRAPHY

Tyler Reid is a Ph.D. candidate in the GPS Research Laboratory working under the guidance of Professor Per Enge and Dr. Todd Walter in the Department of Aeronautics and Astronautics at Stanford University. He received his B.Eng. in Mechanical Engineering from McGill University, Montreal, Canada in 2010 and his M.Sc. in Aeronautics and Astronautics from Stanford University in 2012. He is also an alumnus of the International Space University (ISU) Space Studies Program (SSP) of 2011 held at the Technical University of Graz in Austria. His research interests are in global navigation satellite and augmentation systems, navigation integrity, arctic navigation, orbital mechanics, and space applications.

Todd Walter is a senior research engineer in the GPS Research Laboratory in the Department of Aeronautics and Astronautics at Stanford University. He received his Ph.D. from Stanford in 1993 and has worked extensively on the Wide Area Augmentation System (WAAS). He is currently working on dual-frequency, multi-constellation solutions for aircraft guidance. He received the Thurlow and Kepler awards from the ION. In addition, he is a fellow of the ION and has served as its president.

Per Enge is a Professor of Aeronautics and Astronautics at Stanford University, where he is the Vance and Arlene Coffman Professor in the School of Engineering. Here, he directs the GPS Research Laboratory which develops navigation systems based on the Global Positioning System (GPS). He has been involved in the development of WAAS and LAAS for the Federal Aviation Administration (FAA). He has received the Kepler, Thurlow, and Burka Awards from the ION. He also received the Summerfield Award from the American Institute of Aeronautics and Astronautics (AIAA) as well as the Michael Richey Medal from the Royal Institute of Navigation. He is a fellow of the Institute of Electrical and Electronics Engineers (IEEE), a fellow of the ION, a member of the National Academy of Engineering, and has been inducted into the Air Force GPS Hall of Fame. He received his Ph.D. from the University of Illinois in 1983.

ABSTRACT

The L1 Minimum Operational Performance Standards (MOPS) were designed under the premise that Satellite Based Augmentation Systems (SBAS) be supported by communications satellites in geostationary orbits (GEO). As such, the ephemeris and almanac messages were tailored for this orbit type. However, new satellite orbits ranging from highly eccentric (HEO), inclined geosynchronous (IGSO), medium (MEO) to low Earth (LEO) orbits are being utilized and proposed for Global Navigation Satellite Systems (GNSS) and Satellite Based Augmentation Systems (SBAS). It is thus desirable that the future generation of MOPS ephemeris and almanac messages be able to support these various orbit classes. Such a message has been proposed for the modernized L5 MOPS which is based on an augmented set of Keplerian orbital elements [1]. This paper evaluates this proposed L5 MOPS ephemeris message in terms of the message population in practice. This qualification is based on performance of the population algorithm in terms of functionality, accuracy, failure rate, as well as computational effort as the fitting algorithm must ultimately function to within the limited resources of the WAAS safety computer and other equivalent systems. Case studies using a year of high fidelity orbit data demonstrate the effectiveness of the message for a variety of different GNSS and SBAS orbits including GPS, GLONASS, BeiDou, WAAS, EGNOS, QZSS, NNSS, Cicada/Parus and other proposed orbit classes such as Molniya.

INTRODUCTION

GPS has launched its first five L5 capable satellites (Block IIF) and is slated to achieve its L5 Full Operational Capability (FOC) by the year 2019. GLONASS has returned to a full constellation of 24 operational satellites and has plans to offer CDMA signals at both the L1 and L5 frequencies. The European Galileo and Chinese BeiDou constellations are currently under construction and also intend to broadcast in both the L1 and L5 bands. Thus, it is possible that in the next decade, there could be four constellations suitable for use in

aviation with signals at L1 and L5. The Radio Technical Commission for Aeronautics (RTCA) is developing an update to the Satellite Based Augmentation System (SBAS) Minimum Operational Performance Standards (MOPS) to include the use of GPS L5. The European Organization for Civil Aviation Equipment (EUROCAE) is similarly developing dual frequency MOPS for Galileo. The intent is that these two efforts will be merged into a single MOPS [2].

The different SBAS service providers have formed an Interoperability Working Group (IWG) to ensure that their respective systems remain compatible as well as to plan for future enhancements. This group has set a goal of having the next MOPS support all four constellations [2].

New satellite orbits, ranging from highly eccentric (HEO), inclined geosynchronous (IGSO), medium (MEO) to low Earth (LEO) orbits are being utilized and proposed for GNSS and SBAS constellations. It is desired that in the future, the MOPS integrity message be capable of being delivered by this wide range of orbit classes. This calls for a different ephemeris and almanac message which can handle this broad spectrum of proposed orbital regimes. In the past, the MOPS orbit message used Earth fixed Cartesian position, velocity, and acceleration (9 degrees-of-freedom (DOF)) to describe the motion of the geostationary (GEO) SBAS satellites. The proposed next generation L5 MOPS message will have to be much more sophisticated in order to encompass potential augmentation satellites ranging from GSO to LEO. A method of optimally fitting orbital elements has been devised which allows for a wide variety of orbital elements to be employed. A new 9 DOF set of orbital elements has been selected for the ephemeris message and a 7 DOF set for the almanac which function amicably for the range of orbits in question [1]. It is the goal of this paper to perform a rigorous evaluation of this proposed ephemeris message in terms of the message population in practice.

GNSS & SBAS ORBITS

A multitude of orbits have been employed throughout the history of navigation and augmentation systems. Figure 1 shows past, present, and future navigation and augmentation systems at their nominal operational altitudes. Early satellite navigation systems such as the US Transit (operational from 1964-1996) and Russian Cicada/Parus (operational from 1976-present) were placed in LEO. As such, it is not unimaginable that navigation or augmentation services be offered from LEO in the future. In fact, there has been considerable interest in using the Iridium satellite phone constellation for this very application, for example [3, 4].

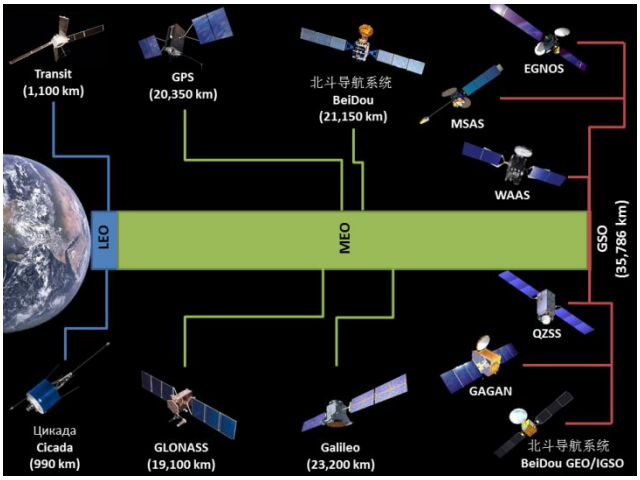

Figure 1: GNSS and SBAS orbit classes

Medium Earth orbits have now been employed by all GNSS systems including the fully operational GPS and GLONASS constellations as well as those of Galileo and BeiDou which are currently in the construction phase. Additional geometry has been added by the BeiDou system via the inclusion of GEO and inclined GSOs (IGSO). Making use of the 24 sidereal hour period of these orbits, these satellites are always over China, giving rise to a regional service with only 10 satellites in the year 2011.

Augmentation systems such as the US WAAS, European EGNOS, and Japanese MSAS, i.e. those which broadcast the L1 MOPS message currently for civil aviation purposes, are placed in GEO. However, new augmentation systems such as Japan's Quasi-Zenith Satellite System (QZSS) offer GPS augmentation to improve geometry for users in cities with tall skyscrapers where the urban canyon effect limits GPS-only performance. QZSS is not only an IGSO it also has a considerable eccentricity which gives rise to the satellite spending most of its time over the northern hemisphere and Japan. Other types of orbits are also being considered for augmentation. Originally used for high latitude communications, highly eccentric orbits (HEO) such as Molniya and Tundra orbits are being considered for Arctic integrity where current SBAS GEOs are below the horizon and cannot be seen [4].

Figure 2 shows all of the trajectories used by GNSS and SBAS today with the inclusion of the Iridium constellation in LEO. This gives a sense of the relative scales of LEO, MEO, and GSO and the vast distances between them. It has been shown that it is possible to design an ephemeris for the L5 MOPS which can describe this wide range of orbit classes [1]. This paper demonstrates the feasibility of implementing this message in practice in terms of message generation algorithms and overall message performance.

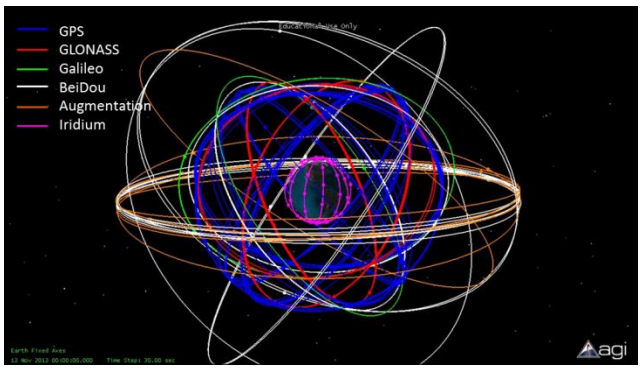

Figure 2: All GNSS satellites and augmentation systems plus the Iridium constellation

L1 MOPS EPHEMERIS PERFORMANCE

In this section, an analysis of data which was provided by the Raytheon Company is performed. This was done in order to gain insight into the current system performance in implementing the L1 MOPS in the Wide Area Augmentation System (WAAS). The data set used here involves one month of message type 9 data which consists of SBAS GEO satellite clock and orbit information, the structure and parameters of which are given in Figures 3 and 4, respectively. Specifically, message type 9 contains the epoch time t_0, User Range Accuracy (URA), a_{Gf0} and a_{Gf1} which describe the GEO satellite clock offset, and the satellite ephemeris in the form of Earth fixed position $\{x_G, y_G, z_G\}$, velocity $\{\dot{x}_G, \dot{y}_G, \dot{z}_G\}$, and acceleration $\{\ddot{x}_G, \ddot{y}_G, \ddot{z}_G\}$.

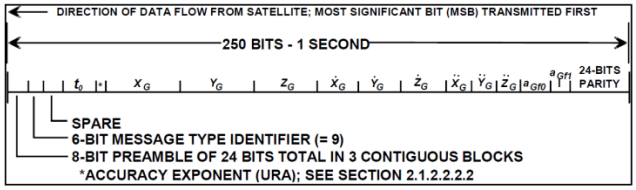

Figure 3: L1 MOPS type 9 GEO navigation message format [5]

Parameter	No. of Bits (Note 1)	Scale Factor (LSB)	Effective Range (Note 1)	Units
Reserved	8			
t_0	13	16	0 to 86,384	seconds
URA (Note 2)	4	(Note 2)	(Note 2)	(Note 2)
X_G (ECEF)	30	0.08	±42,949,673	meters
Y_G (ECEF)	30	0.08	±42,949,673	meters
Z_G (ECEF)	25	0.4	±6,710,886.4	meters
X_G Rate-of-Change	17	0.000625	±40.96	meters/sec
Y_G Rate-of-Change	17	0.000625	±40.96	meters/sec
Z_G Rate-of-Change	18	0.004	±524.288	meters/sec
X_G Acceleration	10	0.0000125	± 0.0064	meters/sec^2
Y_G Acceleration	10	0.0000125	± 0.0064	meters/sec^2
Z_G Acceleration	10	0.0000625	± 0.032	meters/sec^2
a_{Gf0}	12	2^{-31}	$\pm 0.9537\times10^{-6}$	seconds
a_{Gf1}	8	2^{-40}	$\pm 1.1642\times10^{-10}$	seconds/sec

Figure 4: L1 MOPS type 9 GEO navigation message parameters [5]

The current WAAS constellation consists of 3 GEO satellites which emit GPS-like L1 signals with PRN codes 133, 135, and 138. All three are telecommunications satellites, PRN 133 is narrow-band and PRNs 135 and 138 are wide-band. In addition, PRN 133 supports non-precision approach ranging service, whereas PRNs 135 and 138 support en-route though precision approach modes [6]. Table 1 summarizes the attributes and functionality of the current WAAS constellation and Figure 5 shows the orbit groundtracks. It is evident from their groundtracks that PRNs 135 and 138 are in more tightly controlled GEO orbits than that of PRN 133 whose orbital inclination is now at 3 degrees compared to the others each at less than 3 arc minutes. This can also be seen in Figures 6 through 8 which show the satellites' motion with respect to its mean position in the Earth fixed frame. PRN 133 follows the figure-eight track typical of inclined GEO satellites otherwise known as an analemma.

Name	PRN	Lon.	Mfg.	Operator	Support
Inmarsat 4F3 (AMR)	133	98° W	Inmarsat	Inmarsat	non-precision approach ranging service
Galaxy 15 (CRW)	135	133° W	Intelsat	Lockheed Martin	en route through precision approach modes
Anik F1R (CRE)	138	107.3° W	TeleSat	Lockheed Martin	en route through precision approach modes

Table 1: WAAS constellation attributes [6]

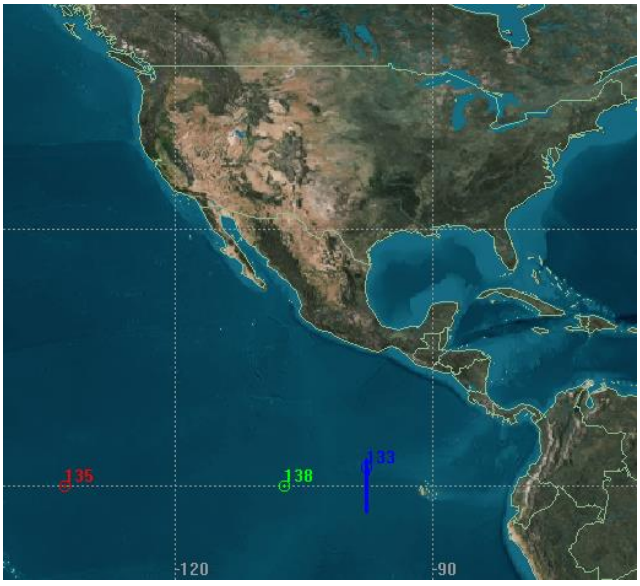

Figure 5: WAAS constellation groundtracks

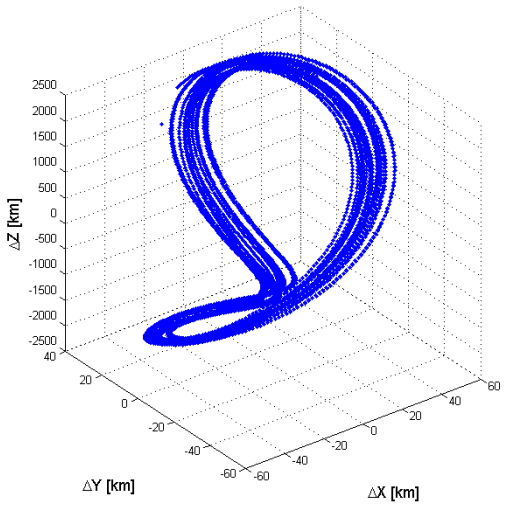

Figure 6: PRN 133 ECEF motion from mean position

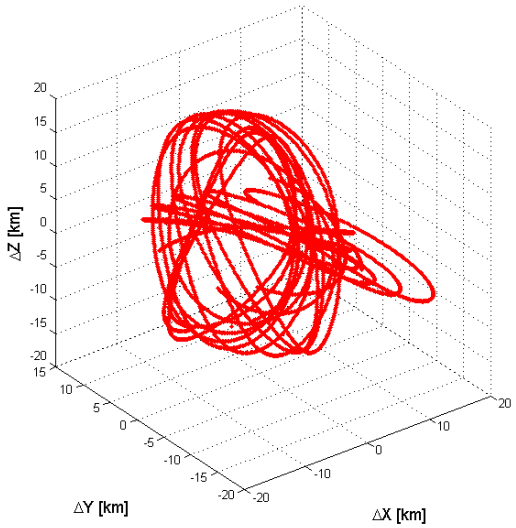

Figure 7: PRN 135 ECEF motion from mean position

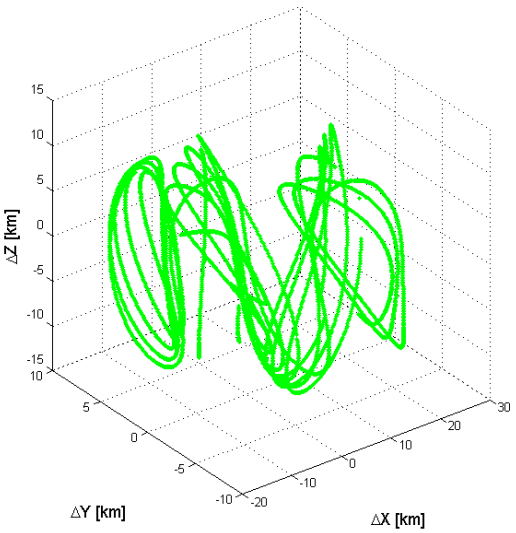

Figure 8: PRN 138 ECEF motion from mean position

The first message parameter examined was the broadcast User Range Accuracy (URA). Figure 9 shows the URA for the WAAS constellation for the time period between March 12, 2013 and April 11, 2013. The gaps in the data are data which were not available to us and in no way represents failures in the system. Here, we see the difference between PRN 133 and PRNs 135/138, the former is typically set to values around 16 – 32 meters and the later are typically set to 2 – 4 meters, thus showcasing the difference between the narrow- and wide-band satellites and their difference in functional capacity, i.e. en route vs. precision approach. There is a similar trend in the satellite clock performance. Figure 10 shows that the clock offset of the wide-band satellites settling around ±70ns compared to that of the narrow-band which settles between ±550ns, a result which is consistent with those presented by the Raytheon Company in [7].

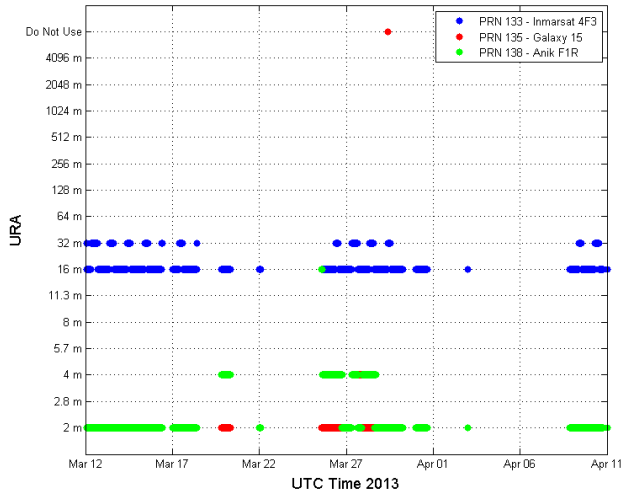

Figure 9: WAAS URA

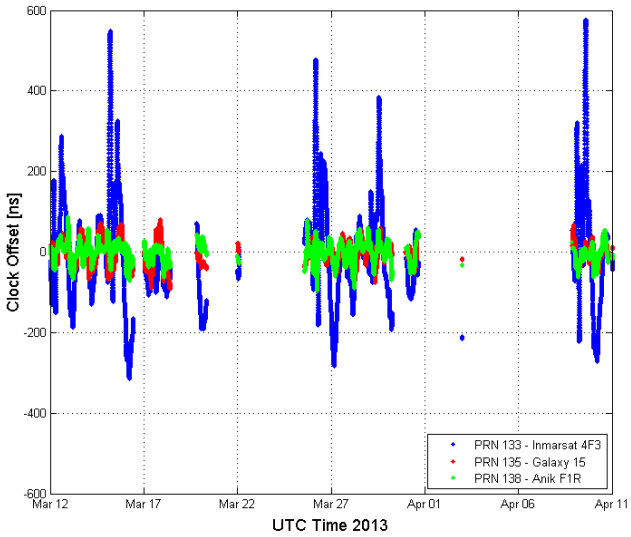

Figure 10: WAAS clock offset

The ephemeris parameters also provided much insight into the system performance. The L1 MOPS ephemeris message is updated and rebroadcast every 60 seconds and is intended to be used for a two minute interval with a potential for coasting up to six minutes with penalty. The satellite position $\mathbf{r}(t)$ is calculated using the aforementioned type 9 parameters use as follows :

$$\mathbf{r}(t) = \begin{bmatrix} x_G \\ y_G \\ z_G \end{bmatrix} + \begin{bmatrix} \dot{x}_G \\ \dot{y}_G \\ \dot{z}_G \end{bmatrix} (t - t_0) + \frac{1}{2} \begin{bmatrix} \ddot{x}_G \\ \ddot{y}_G \\ \ddot{z}_G \end{bmatrix} (t - t_0)^2 \qquad (1)$$

In order to characterize the message performance, we were interested in computing the error growth of this message with time. To examine this, we compared each message in the available data set with subsequent messages for up to a 10 minute interval. These subsequent messages were assumed to be the most up to date and best estimate of the orbit. Figure 11 shows how adjacent messages compare with each other after a period of several minutes. The solid lines represent these values on average and the shaded regions represent the 2σ envelope. The GEO navigation ephemeris message is based on the best estimate the orbit made on the ground. As such, we would expect the uncertainty in the 3D position estimate of the satellite which relies heavily on range measurements to be at least as large as the uncertainty in these measurements. Thus, these messages will inherently include measurement errors which are at least as large as the URA values since these are a reflection of the range measurement uncertainty. For the precision approach capable satellites, PRNs 135 and 138, we see that the message error does not grow substantially over the first 6 minutes as the error is dominated by the URA which is around 2 - 4 meters. Thus, what we are seeing in this data set is the accuracy of the measurements in lieu of the message performance itself. The narrow-band PRN 133 appears to have a more accurate message, but the data here is deceiving. As the satellite is not rated for precision approach ranging service, this is likely not representative of the orbit accuracy but instead the self-consistency in the message generation. This message likely relies less heavily on measurements in its orbit estimate update due to its higher values indicated for URA. As such, this is more representative of the L1 MOPS ephemeris message's ability to describe the best known numerically propagated orbit on the ground produced by the propagation model in the NASA/JPL developed Real-Time GIPSY-OASIS (GPS-Inferred Positioning System - Orbit Analysis and Simulation Software).

The L1 MOPS ephemeris message is limited in accuracy simply due to the quantization of its parameters. Figure 4 shows the message parameters' least significant bit (LSB) which is 8 cm for the X-Y components and 40 cm for the out of plane Z component. Later results will show that these specifications give rise to a message which can convey the orbital position of the satellite to the user to a resolution of 20-40 cm over the 2 minute design life of the message, growing to the meter level at 6 minutes. Figure 12 also shows this result. Here, we have focused on PRN 133 over a period of 6 minutes. Over the first 2 minutes, we find that the message differs from subsequent ones by about 40 cm, a result expected as this is resolution of the message itself. After 6 minutes the message grows to the several meter level, a result which also matches those obtained in modeling WAAS performance (shown later), giving confidence in our implementation of the model, its assessment, and the subsequent comparisons made with the proposed L5 MOPS ephemeris message.

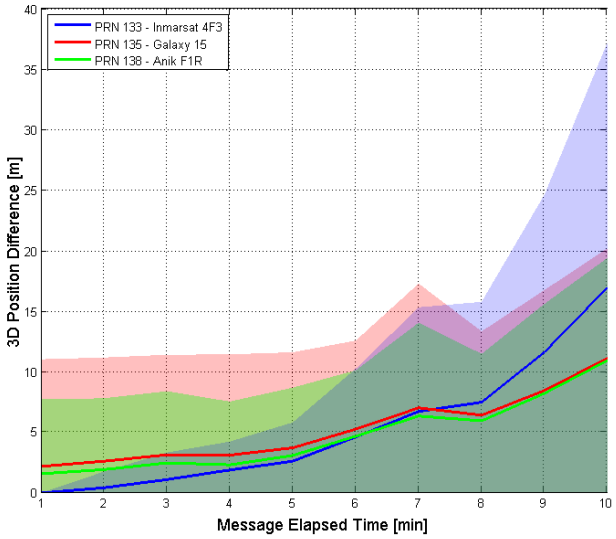

Figure 11: GEO navigation message error growth with time for the WAAS implementation of the L1 MOPS (solid lines represent mean values and shaded regions represent the 2σ envelope)

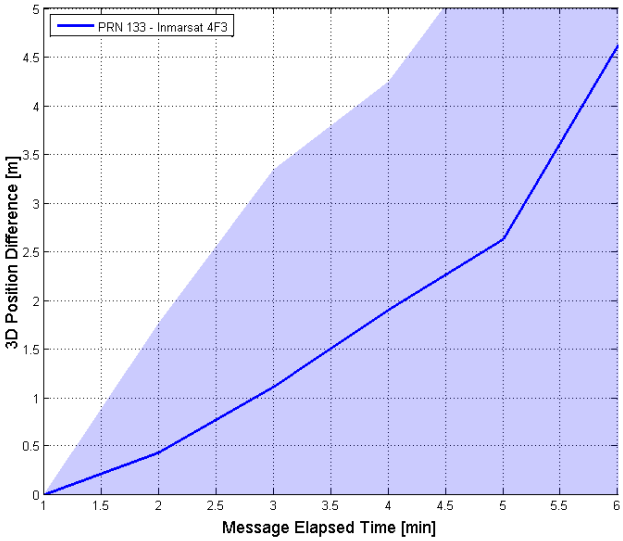

Figure 12: GEO navigation message error growth with time for PRN 133

In summary, these results give insight into the orbit estimators used in practice in WAAS. The precision approach wide-band GEOs likely make heavy use of measurements in producing its orbit updates whereas the narrow-band likely weights these to a lesser extent, thus showcasing the orbit propagator itself and the resolution of the message in practice. In addition, this gives us confidence in our model used in evaluating the L1 MOPS ephemeris message in practice.

L5 MOPS EPHEMERIS MESSAGE OVERVEIW

The proposed L5 MOPS ephemeris message is based on an augmented set of Keplerian orbital elements [1]. Like its predecessor, it remains a 9 degree of freedom parameterization of the orbit and is based on a subset of the GPS ephemeris orbital elements, a description of which can be found in [1, 8]. The message parameters are given in Table 2. It consists of a nominal elliptical trajectory described by the six Keplerian elements, namely, the semi-major axis a, eccentricity e, inclination i_0, right ascension of the ascending node Ω_0, argument of perigee ω, and the mean anomaly M_0, as well as an additional three correction terms, namely, a correction rate in the inclination IDOT, as well as the so-called harmonic correction terms in the along-track direction C_{us} and C_{uc}, which allow us to achieve the necessary orbit representation accuracy. The rate in the inclination allows for cross track correction and the harmonic correction terms, which are a subset of those employed by the GPS ephemeris, allow for along-track correction due to J_2 effects. It was determined that over the time scale of this message the dominant 3D position errors observed in using the six Keplerian elements were in the transverse direction, not radial. To mitigate this, we selected parameters which allowed for additional corrections in the along- and cross-track directions. Further description of these elements and the reason for their selection can be found in [1].

Parameter	Description
a	Semi-Major Axis
e	Eccentricity
i_0	Inclination at Epoch
Ω_0	Right Ascension of Ascending Node at Epoch
ω	Argument of Perigee
M_0	Mean Anomaly at Epoch
IDOT	Rate of Inclination
C_{uc}	Amplitude of Cosine Correction Term to Argument of Latitude
C_{us}	Amplitude of Sine Correction Term to Argument of Latitude

Table 2: L5 MOPS ephemeris parameters

The modernized L5 MOPS proposed in [2] allows for the ephemeris message to be delivered in one and a half messages, the structure of which is given in Figure 13. This is not necessarily how the message will ultimately be packaged; its purpose here is to give an idea of how it could be put together. Furthermore, details about the message bit allocation, dynamic range, and least significant bit (LSB) are given in Table 3. A description of the other parameters contained in the L5 MOPS navigation message which are not related to orbit description can be found in [2]. The six Keplerian elements have dynamic ranges based on their definition. The semi-major axis defines the size of the ellipse and in practice it should never exceed that needed for a GEO satellite. The eccentricity must be $0 \leq e < 1$ for a closed orbit, 0 being a circle and 1 being a parabolic escape trajectory. The inclination can range from an equatorial direct orbit ($i = 0°$) to an equatorial retrograde orbit ($i = 180°$), hence $0 \leq i \leq \pi$. The right ascension angle Ω, argument of perigee ω, and mean anomaly M0 are all angular quantities with full range and can hence vary from $-\pi$ to $+\pi$. The remaining correction terms are not so obvious. These were determined experimentally based on simulations performed for the message qualification. The dynamic range chosen here was selected based on the largest values of these parameters observed with an additional 20% margin.

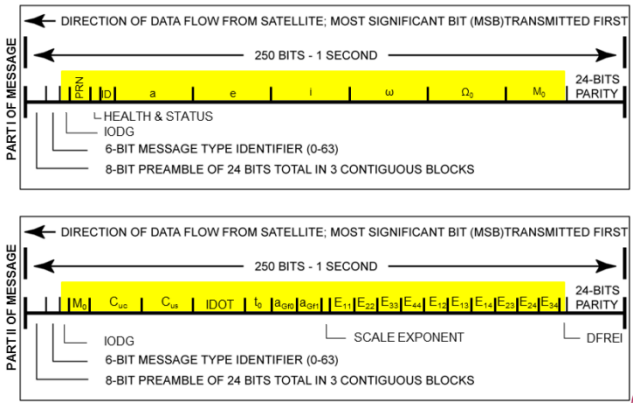

Figure 13: The L5 MOPS SBAS navigation message format

For the L5 MOPS ephemeris message, we set a goal of 3 cm or better resolution over a period of 2 or more minutes and usable, i.e. the message does not grow dangerously erroneous, up to 6 minutes. What is meant by resolution in this context is how well the message conveys the best estimate of the orbit computed on the ground to the end user. The 2-6 minute interval comes for the existing specification in the L1 MOPS and the 3 cm or better resolution comes from a self-imposed target, though is roughly a factor of 10 better than the L1 MOPS in service today.

Parameter	No. of Bits	Scale Factor (LSB)	Effective Range	Units
PRN	8	1	1 – 210	-
IODG × 2	8	1	0 – 16	-
Health & Status	3	-	-	-
Provider ID	4	-	-	-
a	32	0.01	$0 – 4.22\times10^{7}$	m
e	31	2^{-31}	0 – 1	-
i_0	33	$\pi \times 2^{-34}$	$0 – \pi$	rad
Ω_0	35*	$\pi \times 2^{-34}$	$\pm \pi$	rad
ω	35*	$\pi \times 2^{-34}$	$\pm \pi$	rad
M_0	35*	$\pi \times 2^{-34}$	$\pm \pi$	rad
IDOT	22*	1.75×10^{-12}	$\pm 7\pi/6\times10^{-6}$	rad/sec
C_{uc}	20*	3.00×10^{-10}	$\pm \pi/2\times10^{-4}$	rad
C_{us}	20*	3.00×10^{-10}	$\pm \pi/2\times10^{-4}$	rad
Time of day, t_0	13	16	0 - 86,384	sec
a_{Gf0}	12*	0.02	±40.96	m
a_{Gf1}	10*	5×10^{-5}	±0.0256	m/sec
Scale Exponent	3	1	0 – 7	-
$E_{1,1}$	9	1	0 – 511	-
$E_{2,2}$	9	1	0 – 511	-
$E_{3,3}$	9	1	0 – 511	-
$E_{4,4}$	9	1	0 – 511	-
$E_{1,2}$	10*	1	± 512	-
$E_{1,3}$	10*	1	± 512	-
$E_{1,4}$	10*	1	± 512	-
$E_{2,3}$	10*	1	± 512	-
$E_{2,4}$	10*	1	± 512	-
$E_{3,4}$	10*	1	± 512	-
DFREI	4	1	0 – 15	-

*signed value coded as two's compliment

Table 3: L5 MOPS SBAS navigation message parameters

L5 MOPS EPHEMERIS QUALIFICATION

In this section we describe the methods, metrics, and results obtained for the proposed L5 MOPS ephemeris message qualification.

Orbits

In order to perform the message qualification, a representative group of orbits was selected for analysis. A brief discussion of the orbits chosen for analysis, their unique properties, and their reason for selection will be discussed. A summary of the satellites used for analysis and their orbital parameters is given in Table 4.

Satellite	Orbit Class	Period	*e*	*i*
WAAS CRW	GEO	1 Sidereal Day	0	0°
EGNOS Artemis	IGSO	1 Sidereal Day	0	11°
BeiDou IGSO 3	IGSO	1 Sidereal Day	0	55°
QZS-1	IGSO/ HEO	1 Sidereal Day	0.075	40°
GPS PRN 17	MEO	1/2 Sidereal Day	0	55°
GLONASS Cosmos 2461	MEO	8/17 Sidereal Day	0	64°
Molniya 1-93	HEO	1/2 Sidereal Day	0.75	64°
NNSS Oscar 25	LEO	106 min	0	90°
Parus/Cicada Cosmos 2414	LEO	105 min	0	83°

Table 4: Summary of orbits used for analysis

The first satellite chosen for consideration was one the existing SBAS GEOs, namely, the WAAS CRW. Its groundtrack, shown in Figure 14, demonstrates that this is truly a GEO satellite as it is always over the same point on the Earth. This spacecraft has a near zero inclination and is very nearly circular. Next is the EGNOS Artemis satellite shown in Figure 15. This satellite is in a very nearly GEO orbit, though it has a small inclination currently around 10.8°. It turns out that this exceeds the limits of the L1 MOPS ephemeris message. This is largely due to the fact that it is outside the dynamic range of the ECEF Z-component during part of its orbit [1]. This significantly contributed to Artemis being switched to a reduced role in EGNOS. Moving to higher inclination orbits, the BeiDou IGSO-3 is an example of an inclined circular GSO at a 55° inclination (see Figure 16). QZS-1, the first satellite in the Japanese Quazi-Zenith Satellite System (QZSS), is an example of both an inclined and eccentric GSO. This satellite is at a 40° inclination and has an eccentricity of 0.075. This slight eccentricity gives rise to the property that the satellite travels more slowly in the Northern Hemisphere (apogee) and more quickly in the Southern Hemisphere (perigee). This was by design, as the Japanese wanted a satellite that would linger at high elevations over Japan, not give coverage to the Southern Hemisphere.

Moving to MEO, both a GPS and GLONASS orbit were chosen for analysis. GPS satellites are in near circular orbits with an inclination of 55°. Their period of half a sidereal day gives rise to the repeating groundtrack shown in Figure 18. This orbit is similar in many respects to

those of the MEO Galileo and BeiDou satellites. These satellites are in near circular orbits with 55° inclinations, though their orbital periods vary slightly due to European and Chinese systems operating at higher altitudes. These orbital periods are 10/17 and 7/16 of a sidereal for the Galileo and BeiDou systems, respectively. This means that each 10 and 7 sidereal days, the groundtracks will repeat. GLONASS is in a slightly different orbit than other GNSS MEOs. It is again in a near circular orbit, though it is inclined to 63.4°. This was chosen for the J_2 invariant properties of the orbit as well as to give better coverage in Russian high latitude regions. In addition to this, it is at a lower altitude than GPS making it slightly more susceptible to higher order gravity terms. Its orbital period is 8/17 sidereal days, thus its groundtrack (see Figure 19) will repeat in 8 sidereal days.

Another orbit of special interest is the Molniya orbit. Like GPS, Molniya satellites have a repeating groundtrack due to their 12 sidereal hour period, the difference here being that these orbits are highly eccentric (HEO). These satellites were originally designed for communications over high latitude regions of the Soviet Union. In fact, there namesake comes from the original series of satellites used in this orbit, Molniya meaning Lighting in Russian. Like GLONASS, they are inclined to 63.4° in part to provide better coverage at high latitudes but also to make use of the J_2 invariant properties of this inclination. Like QZS-1, its large eccentricity of 0.75 gives the satellite the special property of spending majority of its time over the Northern Hemisphere. This can be seen from the groundtrack shown in Figure 20 where it moves quickly with respect to the Earth in the Southern Hemisphere and then moves more slowly than the Earth and falling behind it in the North. There has been interest in using this type of orbit as a method for delivering navigation integrity to Polar Regions where GEO satellites are not visible [4].

Lastly, LEO navigation satellites from both the US Navy Navigation Satellite System (NNSS) and the Russian Parus/Cicada constellation have been included for analysis. These are circular polar LEO satellites at 1100 km and 990 km altitudes, respectively, with periods of approximately 105 minutes.

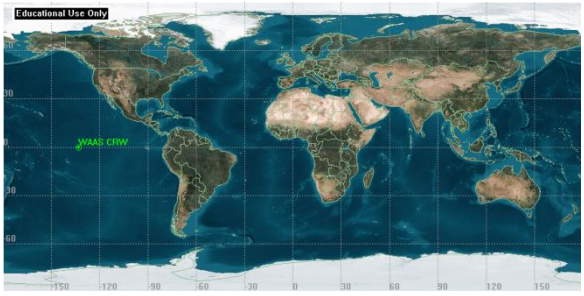

Figure 14: WAAS CRW Groundtrack

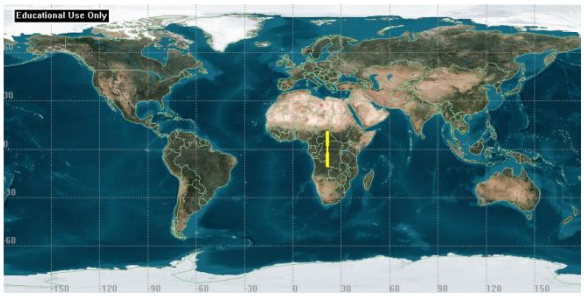

Figure 15: EGNOS Artemis Groundtrack

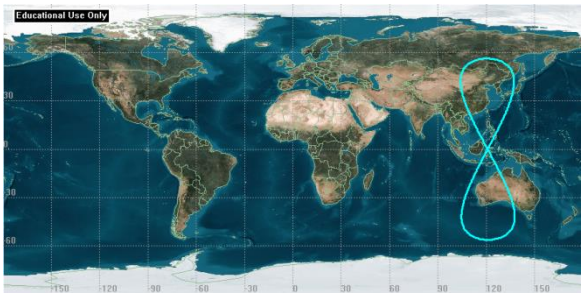

Figure 16: BeiDou IGSO 3 Groundtrack

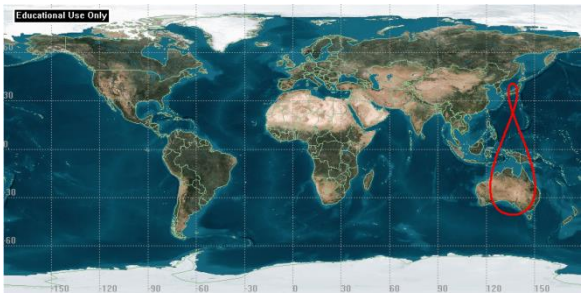

Figure 17: QZS-1 Groundtrack

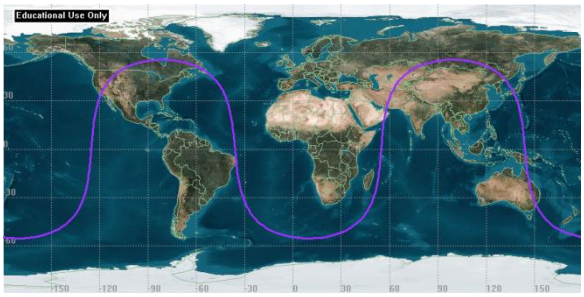

Figure 18: GPS PRN 17 Groundtrack

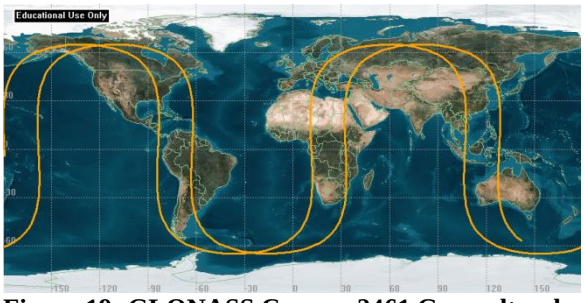

Figure 19: GLONASS Cosmos 2461 Groundtrack

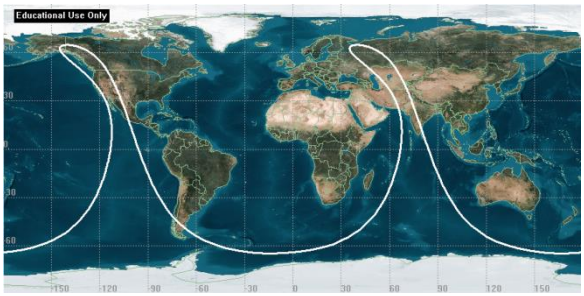

Figure 20: Molniya 1-93 Groundtrack

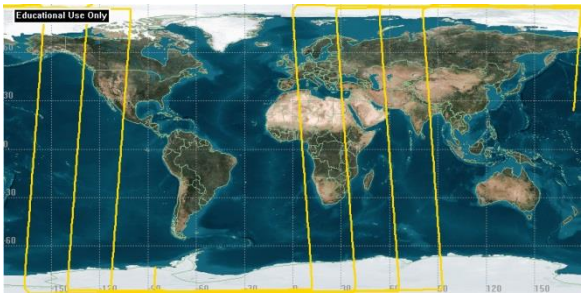

Figure 21: NNSS Oscar 25 Groundtrack

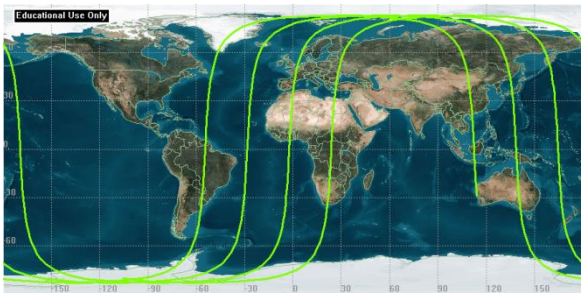

Figure 22: Parus/Cicada Cosmos 2414 Groundtrack

Experimental Methodology

In this section, the experimental methodology and data sets used in the L5 MOPS ephemeris message qualification are described.

In order to rigorously qualify the L5 MOPS ephemeris message, it was generated and then examined at the start of every 30 minute interval for a full year amounting to over 17,000 cases per satellite. The reason for doing this was to ensure that there was no combination of physical effects which could result in fitting algorithm failures or dangerously erroneous messages specific to a time of year. Some orbital perturbations such as gravitational resonances and eclipses seasons have this type of behavior. Eclipse seasons, for example, are the time of year where the shadow cast by the Earth eclipses part of the satellite's orbit. Since the orbit stays nearly fixed in inertial space, the shadow of the Earth will sweep through it over the course of a year, resulting in seasons where force due to solar radiation pressure is effectively turned off during part of the orbit. Figure 23 shows the eclipse seasons for the satellites under consideration. As an interesting aside, COSMOS 2414, part of the Parus/Cicada system, shows what appears to be an anomalous blip in the second half of May. In fact, this represents an eclipse event with the Moon's shadow, further emphasizing the number of different scenarios which can occur. This is only one example of many of the effects which can transpire at specific times, hence the need to evaluate the message population performance at short time steps for the entire year.

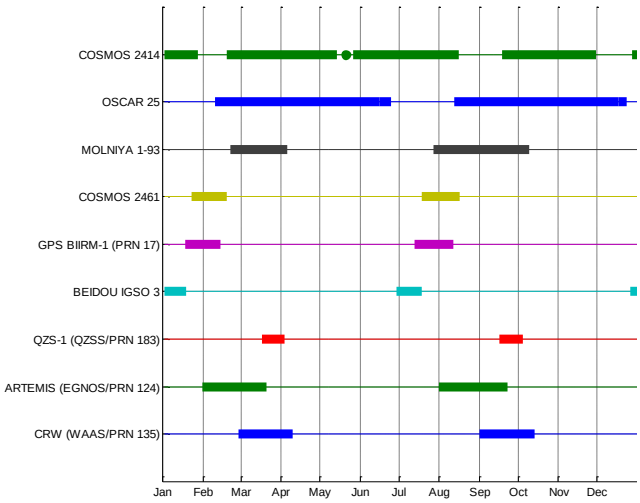

Figure 23: 2012 eclipse seasons

High fidelity orbit trajectory data was needed to both generate the ephemeris message as well as evaluate its performance. Such data is not readily available for the variety of orbits under consideration here (see Table 4). Some high fidelity orbit data does exist from the International GNSS Service (IGS) for GPS and GLONASS satellites [9], however, this does not include the additional orbit regimes in question. Furthermore, IGS orbit data points are spaced at 15 minutes intervals; we require data on the order of seconds in order to fit over intervals of 2-6 minutes. In order to perform this experiment we had to generate our own high-fidelity orbit data which was comparable to the NASA/JPL developed Real-Time GIPSY-OASIS used by WAAS in operation today. For this task, we made use of Analytical Graphics Inc.'s Systems Tool Kit (formerly known as Satellite Tool Kit, both known by the acronym STK). STK's High Precision Orbit Propagator (HPOP) contains similar force models and numerical integration techniques as those employed by GIPSY-OASIS. In previous work [1], STK was used for analysis, however, a simplified orbit model known as the simplified perturbations model SGP4 was used. This semi-analytical model does include many of the dominant orbital perturbations and has its origins in the 1970s where it was to be used in conjunction with the North American Aerospace Defense Command

(NORAD) Two Line Orbital Elements (TLE) [10]. It does not, however, compare to the accuracy of GIPSY-OASIS and is why the switch was made to STK's HPOP. A comparison of the three orbit propagator is given in Table 5. From this, we can see that STK's force models are comparable to those of the GIPSY-OASIS package employed in practice today.

	GIPSY-OASIS [9]	**STK HPOP [11]**	**SGP4 [10]**
Technique	Numerical	Numerical	Semi-Analytical
Earth Gravity Model (Static)	High Order	High Order	J_2, J_3, J_4
Atmospheric Drag	✓	✓	✓
Sun Gravity	✓	✓	✓
Moon Gravity	✓	✓	✓
Solar Radiation Pressure	✓	✓	
Earth Albedo	✓	✓	
Solid/Ocean Tides	✓	✓	
General Relativity	✓	✓	
GPS Attitude Models	✓	✓	

Table 5: Comparison of orbit propagators

Independent comparisons have been performed which demonstrate that the STK HPOP is comparable in accuracy to other industry standard orbit propagators used throughout the history of space operations [12, 13]. A summary and description of these various orbit propagators used can be found in [14]. These validations give further confidence in using STK's HPOP for this analysis as a benchmark for what would be expected to be obtained in practice.

Using STK's HPOP, the experimental high-fidelity data sets were computed as follows:

1. At the epoch time t_0, look up the closest set of available NORAD Two Line Elements.
2. Read this into STK and use the built-in SGP4 orbit propagator to compute the satellite position $\mathbf{r}_0$ and velocity $\mathbf{v}_0$ at t_0. The reason for using SGP4 at this stage is that the TLEs were designed to be compatible with this model. Therefore, this obtains the best estimate of the satellite state at this epoch.
3. This state, along with the spacecraft physical parameters, is fed into STK's HPOP and propagated forward in time for 10 minutes. This yields a data set of sufficient length to perform message fits and error growth analyses. The spacecraft physical parameters necessary here are its mass and area to mass ratio (AMR). An estimate of the mass of the spacecraft is a parameter which is usually easy to look up. The AMR is not usually as readily available but can be estimated from the NORAD TLE's using the method described in [15].

These steps are summarized in the block diagram given in Figure 24. We repeated this for each of the satellites given in Table 4 at the start of each 30 minute interval from January 1st, 2012 00:00:00 UTC to January 1st, 2013 00:00:00 UTC. The reason for the selection of year 2012 is twofold. First, the TLE data for 2012 for each of the satellites of interest is both recent and readily available from [16]. Second, 2012 falls in the predicted solar maximum timeframe [17], thus giving rise to abnormally high levels of solar activity and stronger perturbation forces, exposing the message to some of the more extreme sets of circumstances it should encounter in practice.

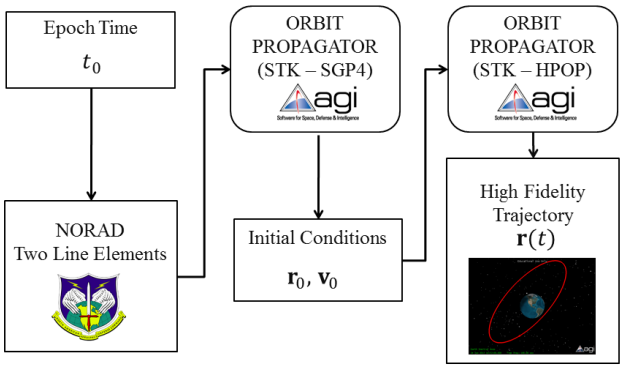

Figure 24: Experimental trajectory generation

Fitting Algorithm Performance

In this section, a description of the fitting algorithm used in the L5 MOPS ephemeris message population is given along with its and the generated message performance.

Generating the orbital elements for the L5 MOPS ephemeris message amounts to solving a nonlinear optimization problem. The end goal is to produce an optimal set of orbital elements $\mathbf{p}^\star$ which offers the best representation of the high-fidelity orbit estimate made by the ground segment to the end user. In previous work [1], this problem was solved via an iterative least-squares (l_2-

norm minimization) scheme. We have since re-cast this problem as both Minimax and l_1-norm minimization problems, each of which would have to be iterated upon to achieve the final solution. It was found that in all cases, iterative least-squares was both more reliable in terms of convergence and also yielded the best result. Thus, the same algorithm in [1] forms the basis of message generation in this work. This algorithm has a tendency to favor the minimization of residuals in the center of the fit interval. To mitigate this effect we introduced a weighting matrix into the least-squares iteration. The process now consists of two steps:

1. Perform the least-squares iterative process described in [1] to obtain an optimal set of orbital elements $\mathbf{p}^\star$.
2. Use the result from Step 1 to compute the residuals at each data point. Use this to form a corresponding weighting matrix **W** based on the error distribution and repeat Step 1 using an iterative weighted least-squares technique with the initial guess being the optimal result from the previous step $\mathbf{p}^\star$.

This revised method ensures that the final residual distribution is more even over the length of the message while maintaining similar algorithm and message performance.

The L5 MOPS ephemeris message qualification consists of two components: (1) an evaluation of the population algorithm (iterative least-squares technique) as well as (2) the final message performance itself. Both of these components are evaluated by generating the L5 MOPS ephemeris message for each of the computed high fidelity orbital trajectories described in the previous section. This allows for the evaluation of both the generation algorithm and final message as depicted in Figure 25.

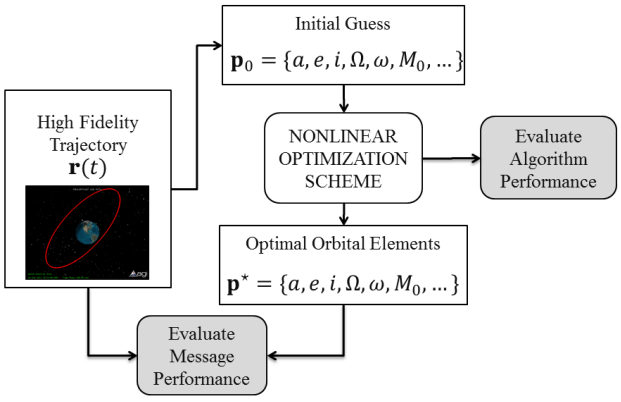

Figure 25: Experimental message generation and qualification

Figure 26 shows the L5 MOPS ephemeris message performance prior to quantization. Each line represents the 3D position error distribution for a particular message generated for one of the cases considered in the year 2012. The abscissa represents the message elapsed time, in this case the message was optimized for a 4 minute interval, and the ordinate represents the 3D position resolution, i.e. how well the message's 9 orbital elements represents the high-fidelity orbital trajectory produced by STK's HPOP. Notice that there is variation as to how well the set of orbital elements represents the actual orbit. This is as expected since the physics of the orbit does change throughout the year. It must be emphasized that this is not the final message which would be distributed to the user as it has not been through the quantization process yet, this will be described in the next section. The purpose of showing these results is to demonstrate the fundamental fit that is obtained from the algorithm so that it can be shown later how much is lost due to quantization. In addition, it should be noted that the IDOT parameter is not included in the parameterization for this GEO case due to problems with algorithm convergence. This is not a difficulty with the algorithm itself, it is instead due to a fundamental problem with describing truly circular equatorial orbits. Only four parameters are needed to describe this case, namely, the semi-major axis *a*, eccentricity *e*, inclination *i*, and an angle known as the true longitude Π which is the angle between the Vernal Equinox and the satellite position in the equatorial plane [18]. In practice, a precisely circular equatorial orbit is very difficult to achieve, though there can be sets of circumstances for tightly controlled GEO orbits, such as WAAS CRW, where they come very close from a numerical standpoint. Therefore, attempting to fit 9 parameters to an orbit which requires only 4 or 5 for description results in problems with the algorithm. We found that excluding the IDOT term for GEO satellites resulted in almost no convergence failures. In all other cases, we experienced no such convergence problems. Figure 27 shows that there was only one convergence failure for all the cases considered for 2012.

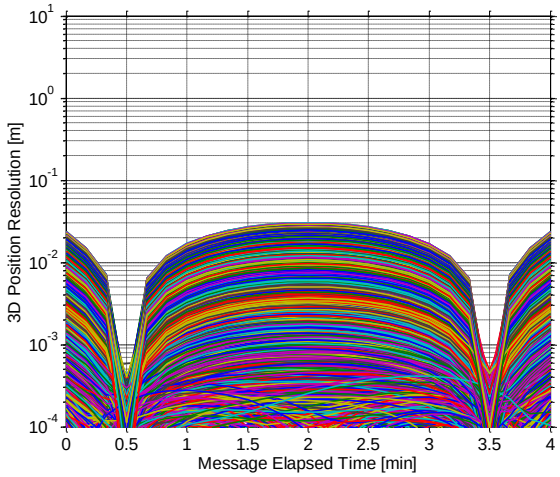

Figure 26: WAAS CRW L5 MOPS ephemeris parameter performance for all 2012 cases

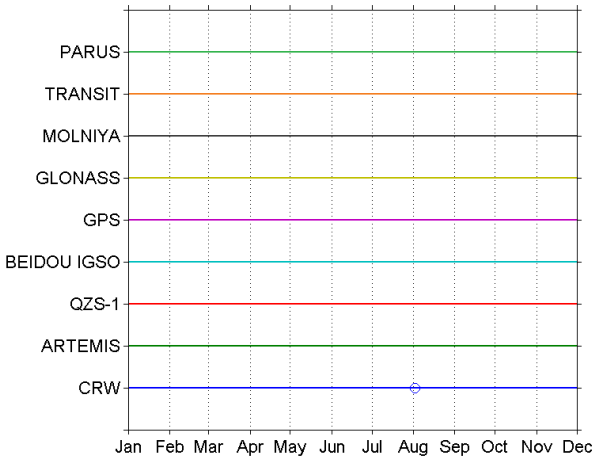

Figure 27: L5 MOPS ephemeris message parameter generation algorithm convergence failures for 2012

The result shown in Figure 26 does not give a sense of the distribution of these fits and how well the message typically describes the orbit. Figure 28 shows a contour plot which helps visualize the distribution of these fits. It shows that, on average, the message parameters can describe the high-fidelity orbit to less than 1 cm, in the tails of the distribution the worst case representation being 3 cm.

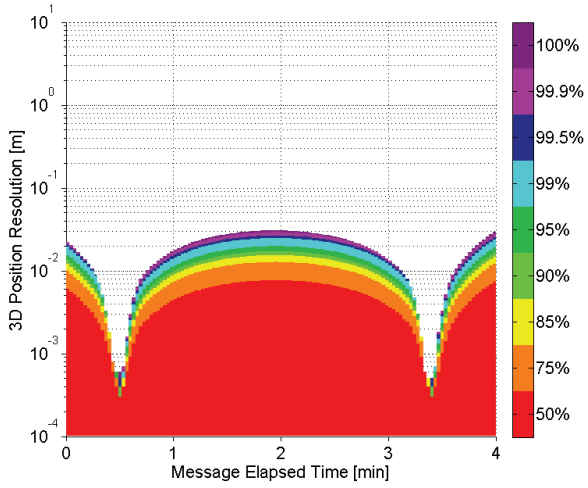

Figure 28: WAAS CRW L5 MOPS ephemeris parameter representation error distribution for 2012

Moving to the slightly inclined GSO Artemis, results shown in Figure 29, we see that on average the message works better in this case than for that of GEO, a representation at the sub millimeter level. The difference here is that all 9 orbital elements are employed, giving rise to more degrees of freedom and hence a better representation. In the tails of the distribution, however, there was one case at the 3 cm level, comparable to the worst case seen in GEO. Both the BeiDou IGSO and QZS-1 show similar performance to Artemis, results of which are given in Figures 30 and 31, respectively. The difference with these cases is that the distribution is somewhat wider, though the worst case representation is similar in the 3 to 4 cm range. The results for the Molniya orbit are similar as well (see Figure 32). In this case, however, the message has been restricted. The reason for this is because during part of its orbit it is very close to the Earth and moving quickly, giving rise to a poor message representation. Assuming the likely scenario where the satellite is used for ranging services around apogee, this is the message performance that would be obtained. This still amounts to 3 to 4 sidereal hours of this 12 sidereal hour orbit.

MEO satellites proved to be more difficult to achieve our stated 3 cm resolution goal over a 4 minute interval even before quantization. To achieve this, we instead optimized for 2 minutes, the length of the L1 MOPS ephemeris message. The results for GPS and GLONASS are given in Figures 33 and 34, respectively. We see similar behavior to that seen in GSO and Molniya, the main difference being the reduced 2 minute timescale.

LEO proved to be the most difficult case. Fitting was done over a 2 minute interval as this is the shortest length the message can be valid for the MOPS. Figures 35 and 36 show the results obtained for Transit and Parus/Cicada, respectively. Both cases have the same nominal behavior, a message representation in the 10 to 20 cm range. Though this is comparable to the L1 MOPS ephemeris message in use today, it does not meet our goal of 3 cm. Though nominally similar to the L1 MOPS, Parus/Cicada showed errors up to 10 meters in the worst case. This raises some serious questions as to the ability to support LEO with this type of message.

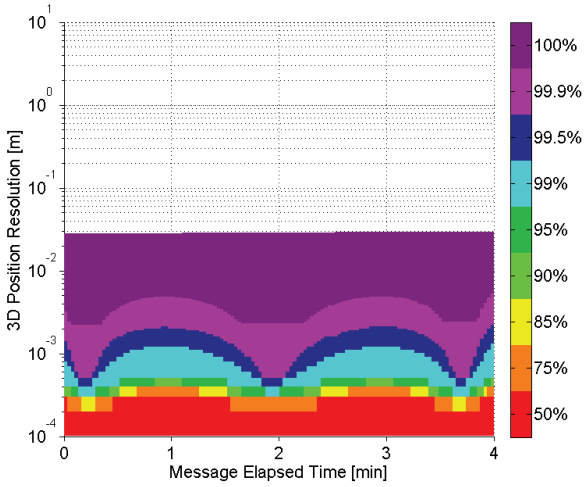

Figure 29: Artemis L5 MOPS ephemeris parameter representation error distribution for 2012

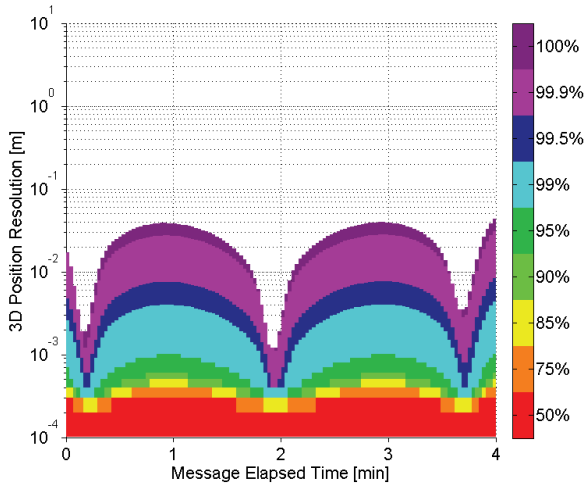

Figure 30: BeiDou IGSO L5 MOPS ephemeris parameter representation error distribution for 2012

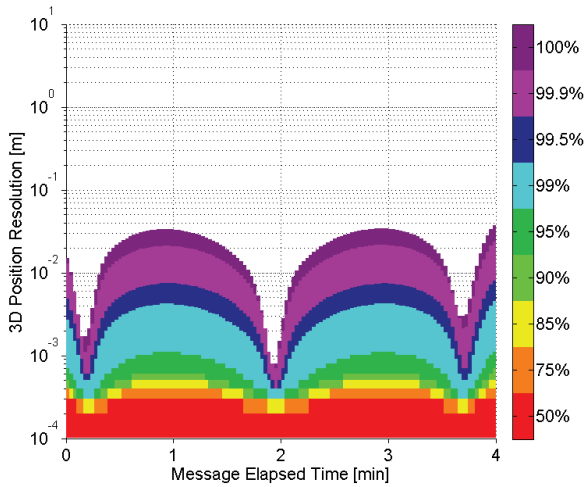

Figure 31: QZS-1 L5 MOPS ephemeris parameter representation error distribution for 2012

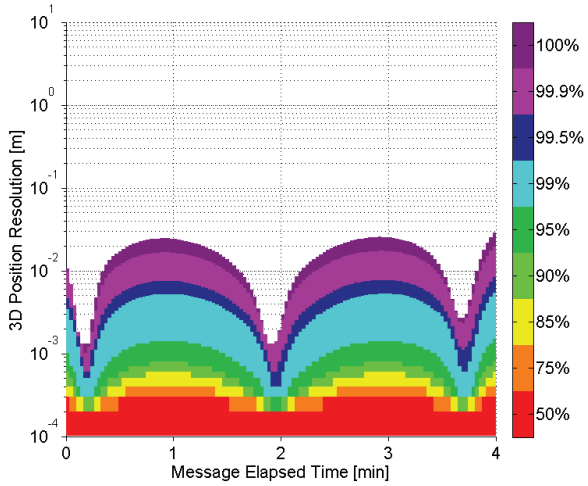

Figure 32: Molniya L5 MOPS ephemeris parameter representation error distribution for 2012

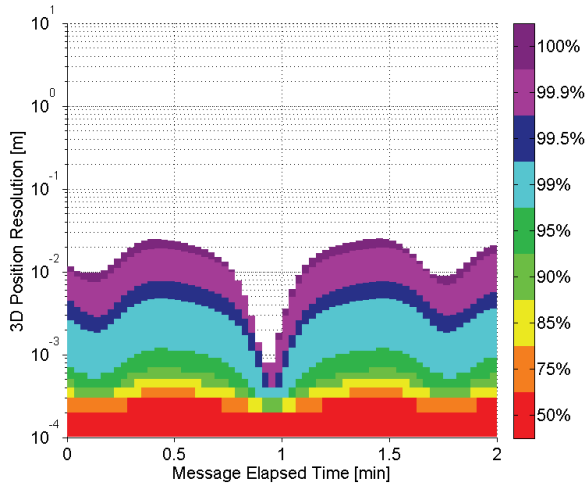

Figure 33: GPS L5 MOPS ephemeris parameter representation error distribution for 2012

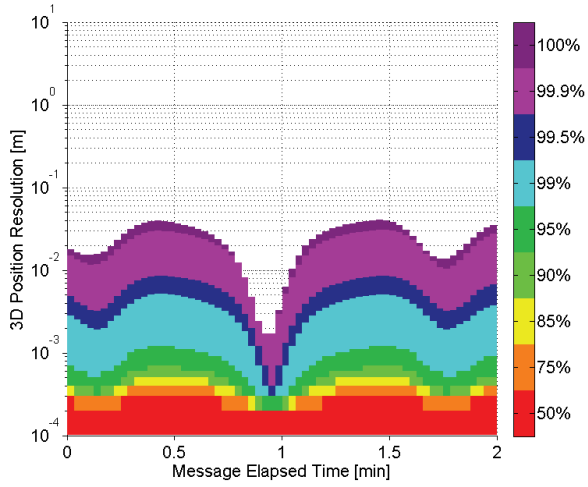

Figure 34: GLONASS L5 MOPS ephemeris parameter representation error distribution for 2012

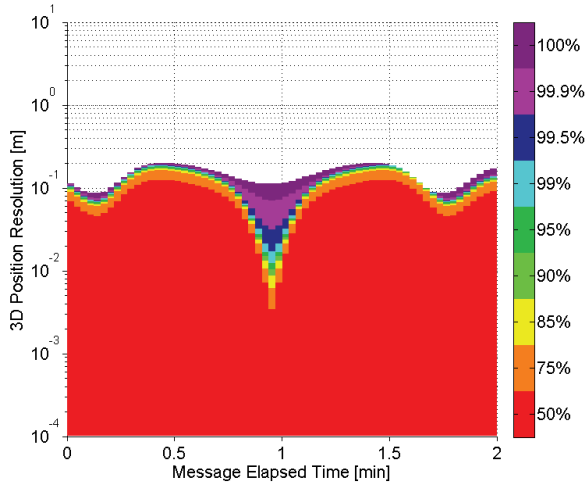

Figure 35: Transit L5 MOPS ephemeris parameter representation error distribution for 2012

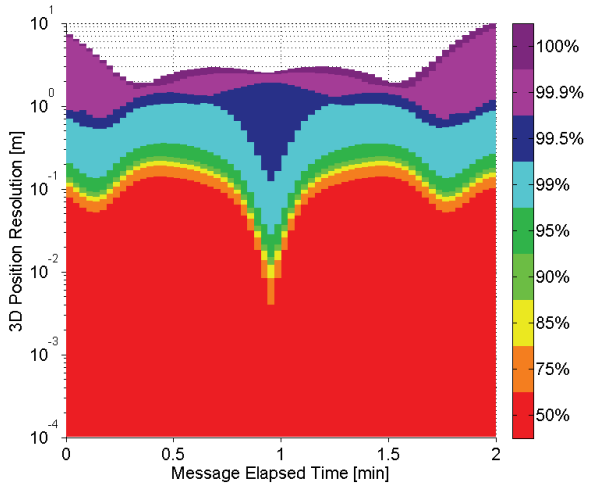

Figure 36: Parus/Cicada L5 MOPS ephemeris parameter representation error distribution for 2012

A summary of message 3D RMS position resolution performance before quantization is given in Figure 37. It is clear that all satellites with the exception of LEO and the special case of an 8 parameter GEO perform comparably well to the sub-centimeter level. This showcases the strength of the parameterization and solidifies that the selection of augmentation parameters, namely, IDOT, C_{us}, and C_{uc} correctly capture the relevant physics in this time scale. Figure 38 shows these cases as a function of time. This plot shows the RMS resolution obtained for all cases considered in the year 2012. Here we see that there is periodicity in the message resolution obtained, the most visible trend being bimonthly. This effect is likely due to lunar gravitational effects. The Moon orbits the Earth with a period of one month in the equatorial plane and during that time will have two points of closest approach with the spacecraft's orbit. These are shown in Figure 39 and are 180° apart, hence the bimonthly periodicity.

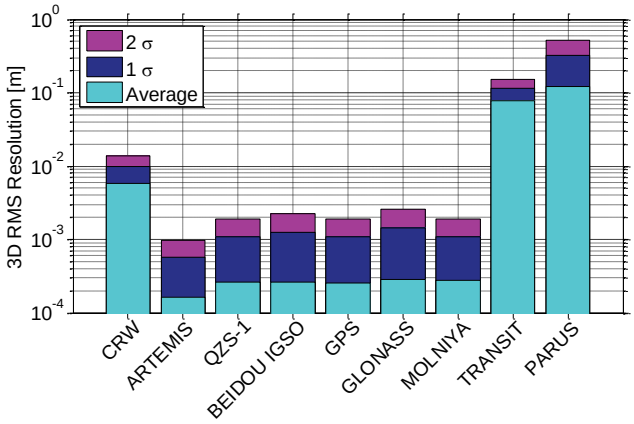

Figure 37: Summary of L5 MOPS ephemeris parameter representation 3D RMS resolution

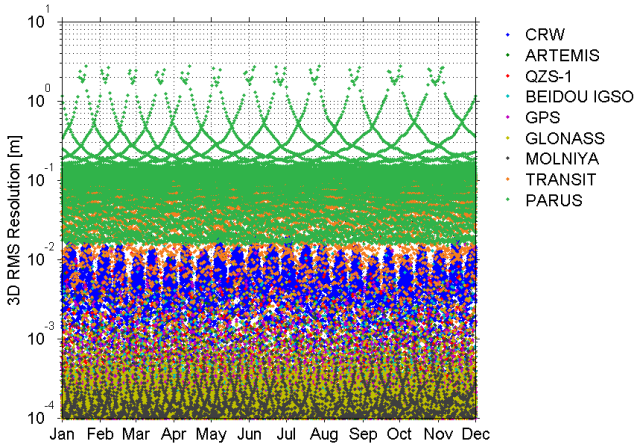

Figure 38: L5 MOPS ephemeris parameter representation 3D RMS resolution as a function of time

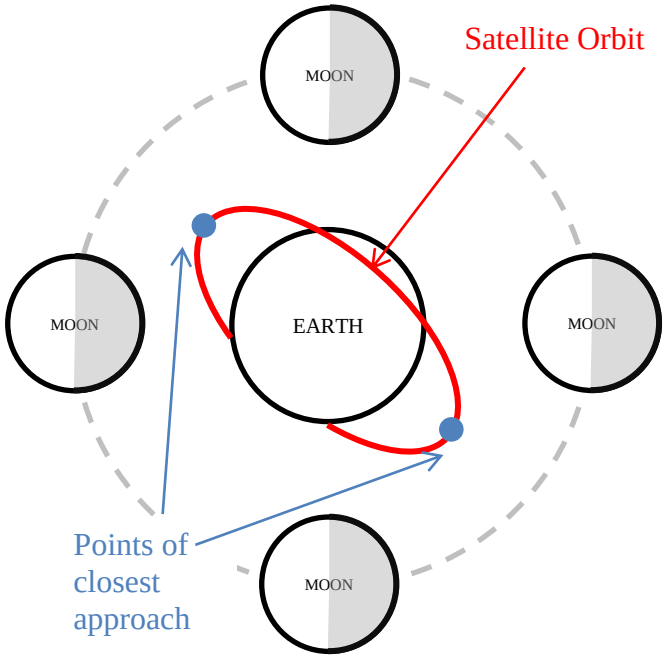

Figure 39: Points of close lunar approach as viewed in the equatorial plane

The final metric is that of computational effort. Ultimately, the message will have to be produced on safety equipment on the ground which can have limited computational resources. From cold start conditions, i.e. no prior knowledge of the orbit, the number of iterations required is summarized in Figure 40 and is typically around 30 or 40 least-squares operations, 80 at most. Notice that it requires more computational effort for Molniya and QZS-1. This is due to the fact that these are orbits of considerably large eccentricity which turns out to be a slightly more difficult problem to solve and thus

requires more iterations to achieve the desired accuracy. In addition, the MEO and LEO satellites required slightly less computational effort compared to their GSO counterparts. The reason for this is that the problem is less sensitive in these regimes and thus easier to solve. The orbital elements to be estimated are angular quantities and at GSO the high altitude results in a large level arm by comparison to MEO and LEO regimes, resulting in higher sensitivity. To give a sense of computation time involved, Figure 41 shows the CPU time required to produce the message normalized with respect to the CPU time required to solve a 4 by 4 linear system, akin to the effort needed to compute a position solution with the minimum number of satellite measurements. This result shows that it requires at most 120 times the amount of time required as it does to compute a simple navigation solution and is well within the computational resources available.

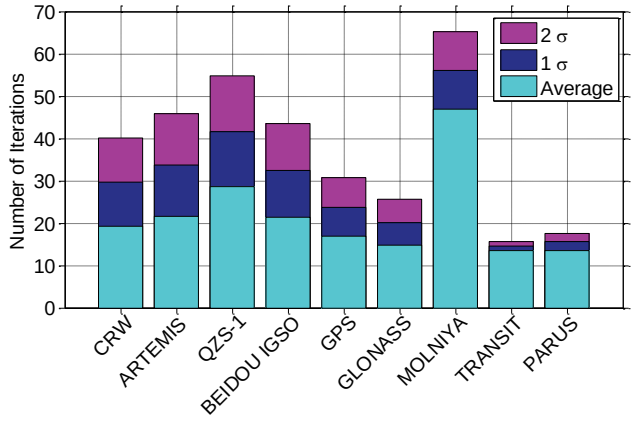

Figure 40: Summary least-squares iterations

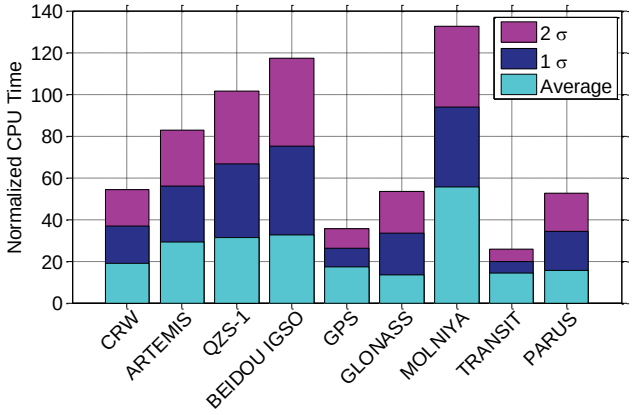

Figure 41: Summary of normalized CPU time

Quantization & Final Message Performance

In this section, the results of the final quantized message performance are given. This is the message that would be distributed to the end user.

The final L5 MOPS ephemeris message is obtained by quantizing the parameters produced in the previous section via the scheme given in Table 3. This table includes, among other things, the dynamic range of the parameters. As discussed previously, the 6 Keplerian elements are quantities that have a dynamic range given by their definition. The dynamic range of the additional correction terms was determined via the multitude of messages produced by this qualification process. The largest magnitude observed of these parameters, with an additional 20% margin, was taken as the dynamic range. Unfortunately, the dynamic range as is does not support all cases in LEO. This decision was made due to the poor performance observed in LEO with this parameterization. Thus, more resources in terms of bit allocation were assigned to support GSO, Molniya, and MEO. The bit allocation was found to be needed in the 6 Keplerian elements over putting more into the correction terms to achieve the necessary accuracy over a wide dynamic range needed to support all orbit classes. As will be shown, the GSO satellites suffered the greatest loss in accuracy due to quantization relative to the original fit. This is due to the fact that at this altitude the orbit has an extremely large lever arm and loss in accuracy in the angular quantities which are the orbital elements is amplified compared to lower altitudes. Thus with a similar quantization scheme, the performance in LEO compared to the previous section would be nearly identical as this case is not as sensitive to degradation in the angular quantities.

Figure 42 shows the quantized message result for the WAAS CRW. This again shows the L5 MOPS ephemeris message error distribution only this represents the final message intended for the end user in its quantized form. Notice that there is not a significant degradation due to quantization compared to the result given in the previous section. Figure 43 shows how this message grows up to the 6 minute mark, its maximum permissible coast time. The message grows up to the 20 cm level by the end of this interval. To give a sense of comparison, Figure 44 shows our implementation of the L1 MOPS ephemeris for the same scenario. This representation now starts at the 20 to 40 cm level simply due to quantization and grows to the 3 to 4 m level by the end of the interval. This agrees with the operational WAAS data given in Figure 12. This indicates a factor of 10 improvement with the proposed L5 MOPS ephemeris message which has the added capacity to represent a multitude of orbit classes with the same fidelity. It is important to emphasize that the 3D position resolution used as a metric here is greater than the error in the user space. In the user space we are interested in the User Range Error (URE), the component of the 3D error projected onto the user space. This is always significantly less since most of the error in the parameterization is in the along-track direction and does not project considerably on to the user.

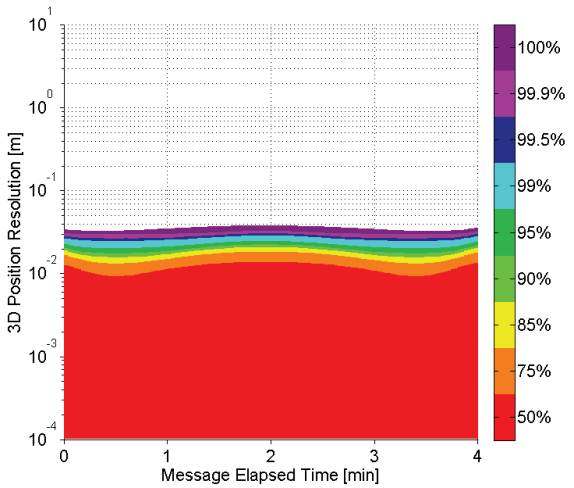

Figure 42: WAAS CRW L5 MOPS ephemeris message error distribution for 2012

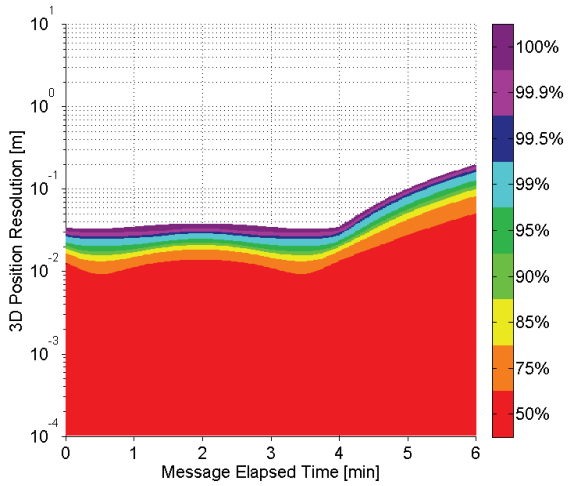

Figure 43: WAAS CRW L5 MOPS ephemeris error growth to 6 minutes

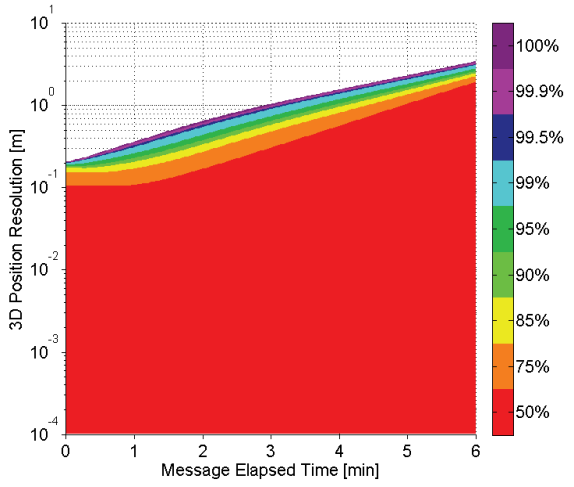

Figure 44: WAAS CRW L1 MOPS ephemeris error growth to 6 minutes

Figure 46 shows the results obtained for Artemis. Notice that the performance is now very similar to the WAAS CRW. Quantization has the effect of flatting the message error, making it even over the length of the message. In addition, quantization has greatly reduced the message's ability to represent the orbit which is theoretically at the sub-millimeter level shown in Figure 29. Quantization has effectively raise the floor of the message's ability to represent the orbit to the 1 cm level, though interestingly has kept the worst cases, around 3 cm, at the same location. Thus, quantization has the effect of raising the accuracy floor while keeping the tails of the distribution the same, effectively shrinking the distribution. It is consistently the same situation for the other scenarios considered, the results of which are given in Figures 47 through 51. These results show that we meet our target of 3 cm resolution or better in 99.9% of cases over the desired time frame of 2 or more minutes. In 100% of cases considered, we reach the 4 cm mark, though results show that this is extremely rare.

Figure 45 shows a summary of the L5 MOPS ephemeris message performance in terms of the 3D RMS resolution. This does not include results for the LEO satellites since they are outside the dynamic range of the quantization scheme. This result shows that that the GSO cases all perform similarly. The MEO and Molniya cases appear to perform better but this is due to the restrictions placed on these messages mentioned earlier. These all perform to the 1 cm RMS or better level on average and the 2 cm RMS level in 95% of cases.

Figure 52 shows the RMS error obtained from all quantized (final) L5 MOPS ephemeris messages produced. This is plotted as function of time to gain insight into differences in message performance throughout the year. Comparing this to the results obtained before quantization, shown in Figure 38, we see that periodic effects are effectively lost in the quantization noise. Again, quantization has effectively raised the accuracy floor while maintaining the tails of the distribution in the same place.

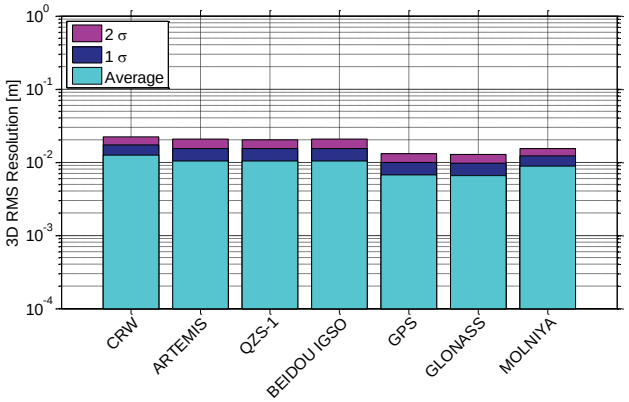

Figure 45: Summary of L5 MOPS ephemeris message 3D RMS resolution

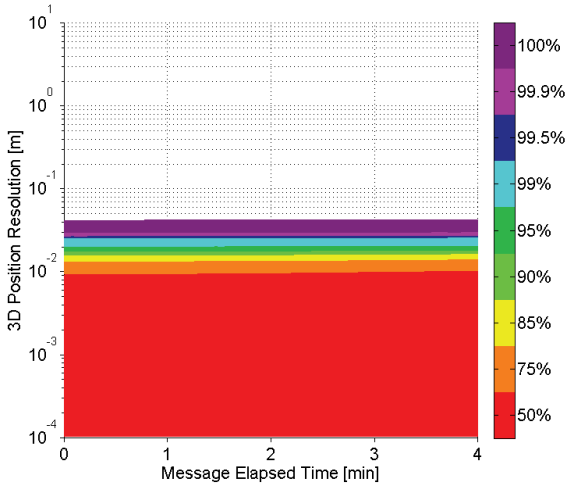

Figure 46: Artemis L5 MOPS ephemeris message error distribution for 2012

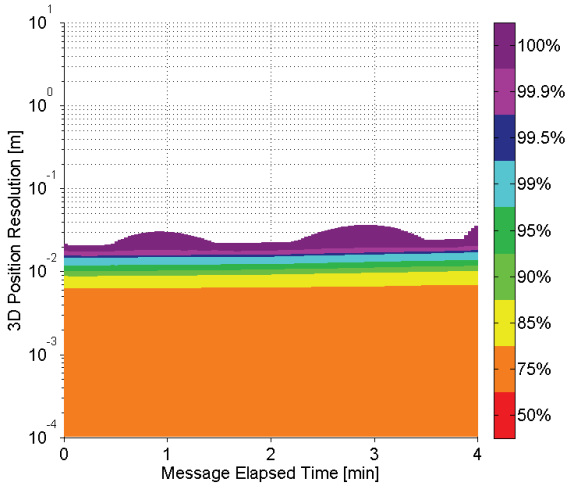

Figure 49: Molniya L5 MOPS ephemeris message error distribution for 2012

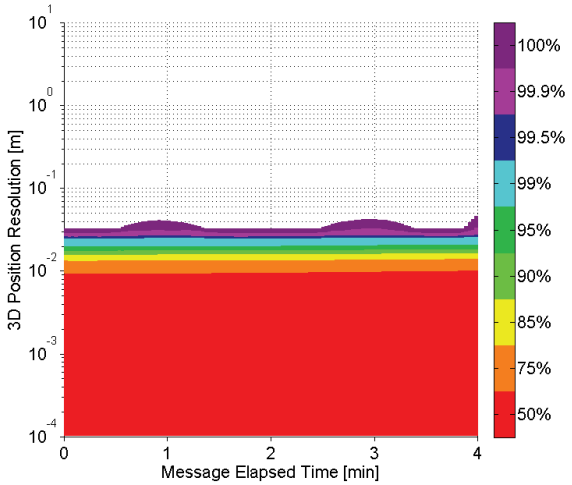

Figure 47: BeiDou IGSO L5 MOPS ephemeris message error distribution for 2012

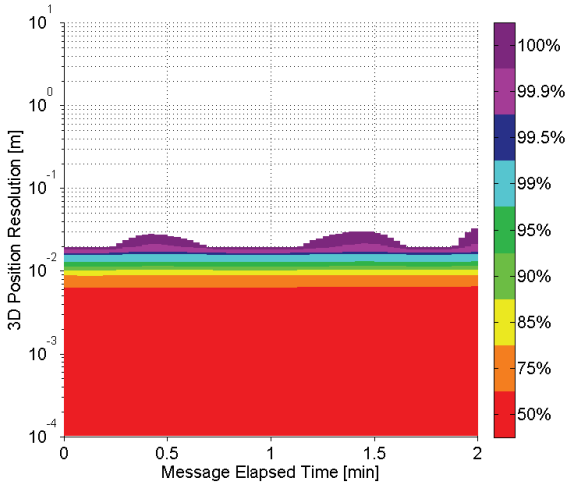

Figure 50: GPS L5 MOPS ephemeris message error distribution for 2012

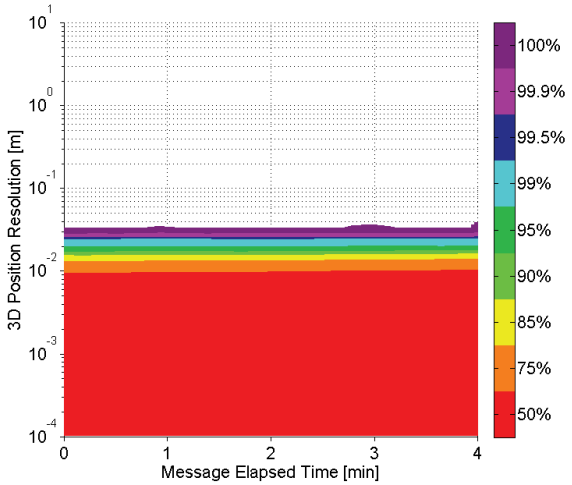

Figure 48: QZS-1 L5 MOPS ephemeris message error distribution for 2012

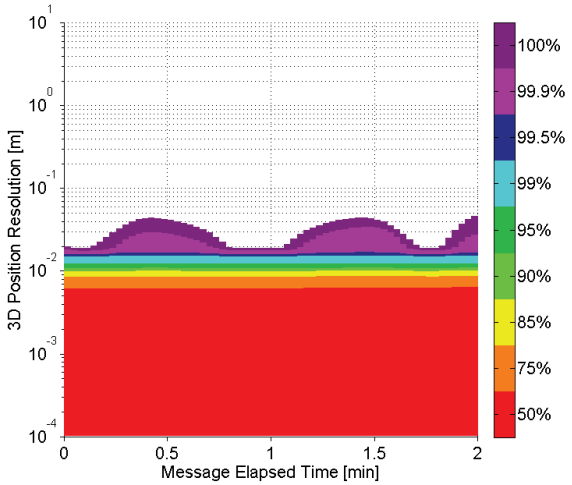

Figure 51: GLONASS L5 MOPS ephemeris message error distribution for 2012

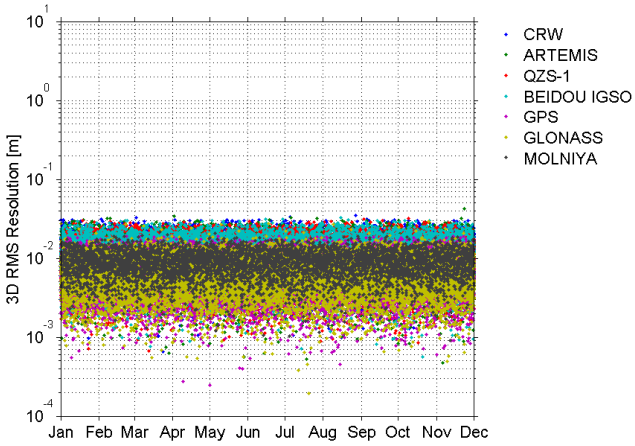

Figure 52: L5 MOPS ephemeris message 3D RMS resolution as a function of time

CONCLUSIONS

In conclusion, the proposed L5 MOPS ephemeris message and population algorithm have been shown to function amicably as a representation method for satellites in a variety of orbit classes which are currently used by GNSS and SBAS systems as well as some which have been proposed for the future. These include GEO, GSO, IGSO, HEO, and MEO.

The population algorithm based on iterative least squares has been shown to be extremely robust with only 1 convergence failure observed in all cases examined for 2012. In addition, the computational effort required is within the capabilities of the ground segment even for cold start conditions where no previous knowledge is known about the orbital parameters to be estimated.

The L5 MOPS architecture allows for the message to be delivered in two message blocks. This message is valid for a period of 4 minutes for GSO and HEO and 2 minutes for MEO. The parameterization is based on an augmented set of orbital elements. This consists of the six Keplerian elements as well as an additional three corrections terms giving rise to cross- and along-track corrections. The message quantization scheme allows for the ground estimated orbit to be represented to within a resolution of 3 cm in 99.9% of cases, 4 cm in all cases observed. This improved accuracy represents a factor 10 improvement over the current L1 MOPS ephemeris message.

Though it takes more bits to convey the information for the L5 ephemeris compared to its L1 predecessor, the advantage is that a broader class of satellite orbits can be supported and thus more satellites can be considered for GNSS integrity applications in the future.

ACKNOWLEDGMENTS

The authors would like to gratefully acknowledge the FAA Satellite Product Team for supporting this work under Cooperative Agreement 2008-G-007. In addition, we would like to also gratefully acknowledge the Raytheon Company and specifically Tim Schempp for providing us with operational WAAS data for analysis.

The opinions expressed in this paper are the author's and this paper does not represent a government position on the future development of L1/L5 WAAS.

REFERENCES

[1] T. Reid, T. Walter, and P. Enge, "L1/L5 SBAS MOPS Ephemeris Message to Support Multiple Orbit Classes," in *Proceedings of the 2013 International Technical Meeting of The Institute of Navigation*, San Diego, CA, 2013.

[2] T. Walter, J. Blanch, and P. Enge, "L1/L5 SBAS MOPS to Support Multiple Constellations," in *Proceedings of the 25th International Technical Meeting of the Satellite Division of the Institute of Navigation (ION GNSS)*, Nashville, TN, 2012.

[3] G. X. Gao, L. Heng, T. Walter, and P. Enge, "Breaking the Ice: Navigating in the Arctic," in *Proceedings of the 24th International Technical Meeting of the Satellite Division of the Insitute of Navigation (ION GNSS)*, Portland, OR, 2011.

[4] T. Sundlisaeter, T. Reid, C. Johnson, and S. Wan, "GNSS and SBAS System of Systems: Considerations for Applications in the Arctic," in *63rd International Astronautical Congress*, Naples, Italy, 2012.

[5] Radio Technical Commission for Aeronautics, *Minimum Operational Performance Standards for Global Positioning System / Wide Area Augmentation System Airborne Equipment, RTCA DO-229D*. Washington, D.C., 2006.

[6] (August 2013) The Almanac: Orbit Data and Resources on Active GNSS Satellites. *GPS World*.

[7] M. S. Grewal, W. Brown, R. Lucy, and P. Hsu, "GEO Uplink Subsystem (GUS) Clock Steering Algorithms Performance, Validation, and Test Results," in *31st Annual Precise Time and Time Interval (PTTI) Meeting*, Dana Point, CA, 1999.

[8] Global Positioning System Directoriate, *Navstar GPS Space / Navigation User Interfaces, Interface Specification IS-GPS-200, Revision F*, 2011.

[9] J. M. Dow, R. E. Neilan, and C. Rizos, "The International GNSS Service in a changing landscape of Global Navigation Satellite Systems," *Journal of Geodesy*, vol. 83, pp. 191-198, 2009.

[10] T. S. Kelso, F. R. Hoots, and R. L. Roehrich, *Space Track Report #3*: U.S. Air Force: Aerospace Defense Command, 1988.

[11] Analytical Graphics Inc. (2011) Satellite Tool Kit Documentation, Version 9.2.2.

[12] C. C. Chao, J. W. Cook, J. Cox, T. F. Starchville, R. C. Thompson, and L. F. Wagner, "Independent Verification and Validation for Analytical Graphics, Inc. of Three Astrodynamic Functions of the Satellite Tool Kit: Version 4.1.0," The Aerospace Corporation ATR-2000(7605)-1, 2000.

[13] D. A. Vallado, "An Analysis of State Vector Propagation Using Differing Flight Dynamics Programs," in *Paper AAS 05-199 presented at the AAS/AIAA Space Flight Mechanics Conference*, Copper Mountain, CO, 2005.

[14] J. R. Vetter. (2007) Fifty Years of Orbit Determination: Development of Modern Astrodynamics Methods. *Johns Hopkins APL Technical Digest*. 239-252.

[15] J. Sang, J. C. Bennett, and C. H. Smith, "Estimation of ballistic coefficients of low altitude debris objects from historical two line elements," *Advances in Space Research*, pp. 117-124, 2013.

[16] T. S. Kelso. (2012). *Celestrack*. Available: http://celestrak.com/

[17] D. H. Hathaway. (2013). *Solar Cycle Prediction*. Available: http://solarscience.msfc.nasa.gov/predict.shtml

[18] D. A. Vallado, *Fundamentals of Astrodynamics and Applications*, 3rd ed. Hawthorne, CA: Microcosm Press, 2007.